556

RADIATION PRESSURE FORCES, THE ANOMALOUS ACCELERATION, AND CENTER OF MASS MOTION FOR THE TOPEX/POSEIDON SPACECRAFT

COLORADO CENTER FOR ASTRODYNAMICS RESEARCH

FINAL REPORT
JPL CONTRACT #1214025
"FY 2000 POD ALGORITHM"

SEPTEMBER 30, 2000

RADIATION PRESSURE FORCES, THE ANOMALOUS ACCELERATION, AND CENTER OF MASS MOTION FOR THE TOPEX/POSEIDON SPACECRAFT

Daniel G. Kubitschek[†] and George H. Born[‡]

Shortly after launch of the TOPEX/POSEIDON (T/P) spacecraft (s/c), the Precision Orbit Determination (POD) Team at NASA's Goddard Space Flight Center and the Center for Space Research at the University of Texas, discovered residual alongtrack accelerations which were unexpected. Here, we describe the analysis of radiation pressure forces acting on the T/P s/c for the purpose of understanding and providing an explanation for the anomalous accelerations. The radiation forces acting on the T/P solar array, which experiences warping due to temperature gradients between the front and back surfaces, are analyzed and the resulting alongtrack accelerations are determined. Characteristics similar to those of the anomalous acceleration are seen. This analysis led to the development of a new radiation force model, which includes solar array warping and a solar array deployment deflection of as large as 2°. As a result of this new model estimates of the empirical alongtrack acceleration are reduced in magnitude when compared to the GSFC tuned macromodel and are less dependent upon β', the location of the sun relative to the orbit plane. If these results are believed to reflect the actual orientation of the T/P solar array, then motion of the solar array must influence the location of the s/c center of mass. Preliminary estimates indicate that the center of mass can vary by as much as 3 centimeters (cm) in the radial component of the s/c's position due to rotation of the deflected, warped solar array panel. The altimeter measurements rely upon accurate knowledge of the center of mass location relative to the s/c frame of reference. Any radial motion of the center of mass directly affects the altimeter measurements.

INTRODUCTION

A few months after launch of the TOPEX/POSEIDON (T/P) spacecraft (s/c), the Precision Orbit Determination (POD) Team at NASA's Goddard Space Flight Center (GSFC) and the Center for Space Research at the Univeristy of Texas, observed residual alongtrack accelerations that were unexpected and of unknown origin[1]. Figure 1 shows the residual alongtrack accelerations for both the GSFC prelaunch macromodel and the GSFC tuned macromodel (nonconservative force model was "tuned" using on-orbit observations up to and including cycle 16). These accelerations represent the residual constant alongtrack accelerations, which are estimated in the orbit determination process

[†]Research Associate, Colorado Center for Astrodynamics Research (CCAR), Aerospace Engineering Sciences, University of Colorado. Email: daniel.kubitschek@Colorado.EDU, Phone: 303 492-7330.
[‡]Director, Colorado Center for Astrodynamics Research (CCAR), Aerospace Engineering Sciences, University of Colorado. Email: george.born@Colorado.EDU, Phone: 303 492-6677.

at a once per day frequency. In addition, alongtrack and crosstrack accelerations, which vary sinusoidally at a frequency of 1 cycle per satellite revolution (one cycle per revolution or 1 CPR), were estimated in the orbit determination process. These residual accelerations have the largest effect upon the orbit solution[2]. The daily average constant alongtrack acceleration shown in figure 1 was termed the "anomalous acceleration" by the POD Team. The solid vertical lines represent yaw mode transitions, the horizontal dashed lines represent the transition to/from full sun orbits (when $|\beta'| > 55.7°$ the s/c is illuminated throughout the entire orbit; below that value the s/c experiences periods of Earth occultation during each orbit). Superimposed upon the residual alongtrack acceleration is a plot of the β' angle during this period. This figure shows that these residual alongtrack accelerations display a dependence upon both the attitude steering mode and/or the sun-orbit geometry.

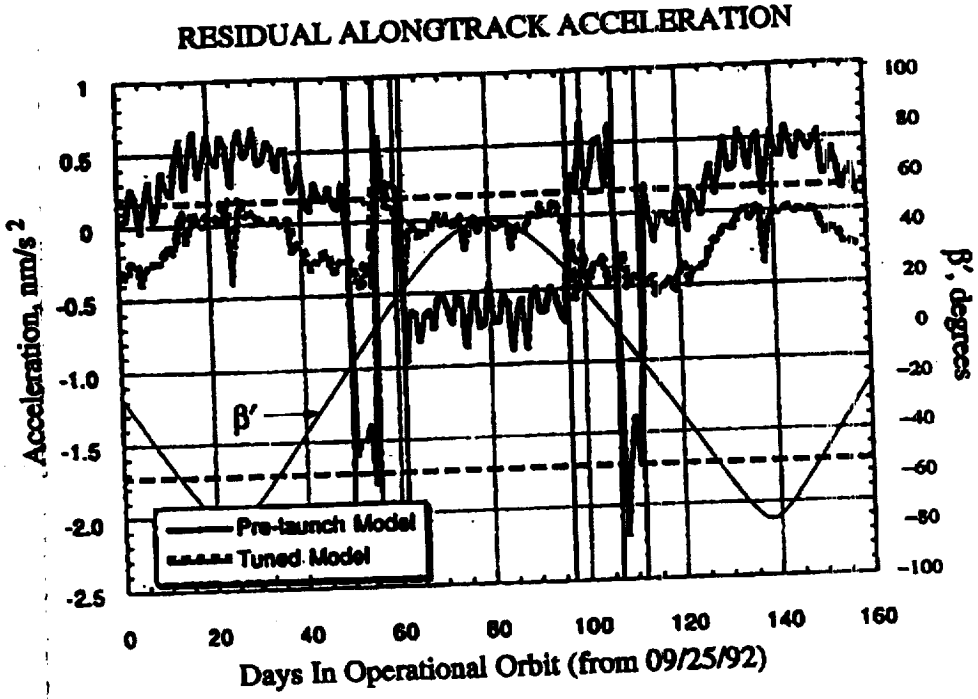

Figure 1 Daily average constant alongtrack accelerations for the first 160 days of the TOPEX/POSEIDON mission.

T/P orbits in one of four distinct yaw modes, depending upon the value of β'. Table 1 shows the yaw steering algorithm for T/P that is required to simultaneously maintain orientation of the altimeter antenna boresight in the nadir (Earth pointing) direction and orientation of the solar array cell side normal vector relative to the sun-line direction vector. β' represents the angle between the sun-line direction vector and the orbital plane, the angle Θ is defined as the orbit angle relative to the sunrise direction vector, and the

angle Ψ specifies the s/c yaw angle (rotation about the $z_{s/c}$ axis of the s/c frame of reference).

Table 1
TOPEX/POSEIDON YAW STEERING ALGORITHM

Yaw Mode	β' Region	Yaw Angle
Orbit Forward Sinusoidal	$\beta' > +15°$	$\Psi = 90° + (90° - \beta')\cos\Theta$
Orbit Forward Fixed	$+15° \geq \beta' > 0°$	$\Psi = 0°$
Orbit Backward Fixed	$0° > \beta' \geq -15°$	$\Psi = 180°$
Orbit Backward Sinusoidal	$-15° > \beta'$	$\Psi = -90° - (90° + \beta')\cos\Theta$

In precise orbit determination of altimetric s/c, the radial component (or height component) of the s/c's location is the most important since orbit errors associated with this component directly affect the altimeter measurement. During the conceptual phase of the mission, two major efforts were launched to improve the predicted orbit precision: (1) development of an improved gravity field model[3] and (2) development of a detailed radiation force model for the T/P s/c[4]. Antreasian and Rosborough (1992) developed and analyzed a prelaunch micromodel approximation of the T/P s/c, which incorporated the complex s/c geometry and attitude steering profile to determine thermal history information for each surface. The acceleration profiles due to incident solar radiation pressure, Earth albedo and infrared emission, and thermal emission of radiation from each surface of the s/c were computed for various values of β'. This micromodel was too computationally intensive for operational orbit determination, but provided the necessary information needed for development of a much simplified radiation force model.

The POD Team used the accelerations from the micromodel analysis to derive a macromodel approximation known as the "box-wing" model. This model consists of eight surfaces, each having a set of property parameters which were adjusted so that the resulting accelerations matched the micromodel accelerations[5]. Figure 2 shows the evolution of the T/P nonconservative force model.

Upon observation of the anomalous acceleration, deficiencies in the macromodel were immediately suspected. Solar array warping was known to exist prior to launch, but thought to be negligible. In order to gain some insight it is important to understand the orientation of the s/c during each of the yaw steering modes. During the orbit forward fixed yaw mode the s/c remains fixed relative to the orbit frame of reference (defined to be the local vertical local horizontal frame) with the $+x_{s/c}$ axis pointing in the direction of the local horizontal direction vector (the projection of the velocity vector onto the local horizontal direction vector is positive). This orientation represents a yaw angle of 0°. During the orbit backward fixed yaw mode, the yaw angle remains fixed at 180°. The sinusoidal yaw modes are more complicated. During the orbit forward sinusoidal yaw mode, the $-y_{s/c}$ axis of the spacecraft oscillates back and forth across the direction of the local horizontal while the amplitude of oscillation varies as a function of β'. The orbit backward sinusoidal yaw mode has the $-y_{s/c}$ axis oscillating about the anti-horizontal direction vector. Here, warping of the solar array or a deployment deflection of the solar array could be responsible for residual alongtrack accelerations. If it is assumed that the solar array is flat, then only the area associated with its thickness would be projected in

the alongtrack direction when $\Psi = 90°$. Inducing curvature increases that projected area and redirects the radiation forces acting on the solar array surface resulting in a deceleration of the s/c. During periods when $\Psi = -90°$, the panel trails the s/c as it moves in orbit about the Earth. In this case the redirected radiation forces would act to accelerate the s/c.

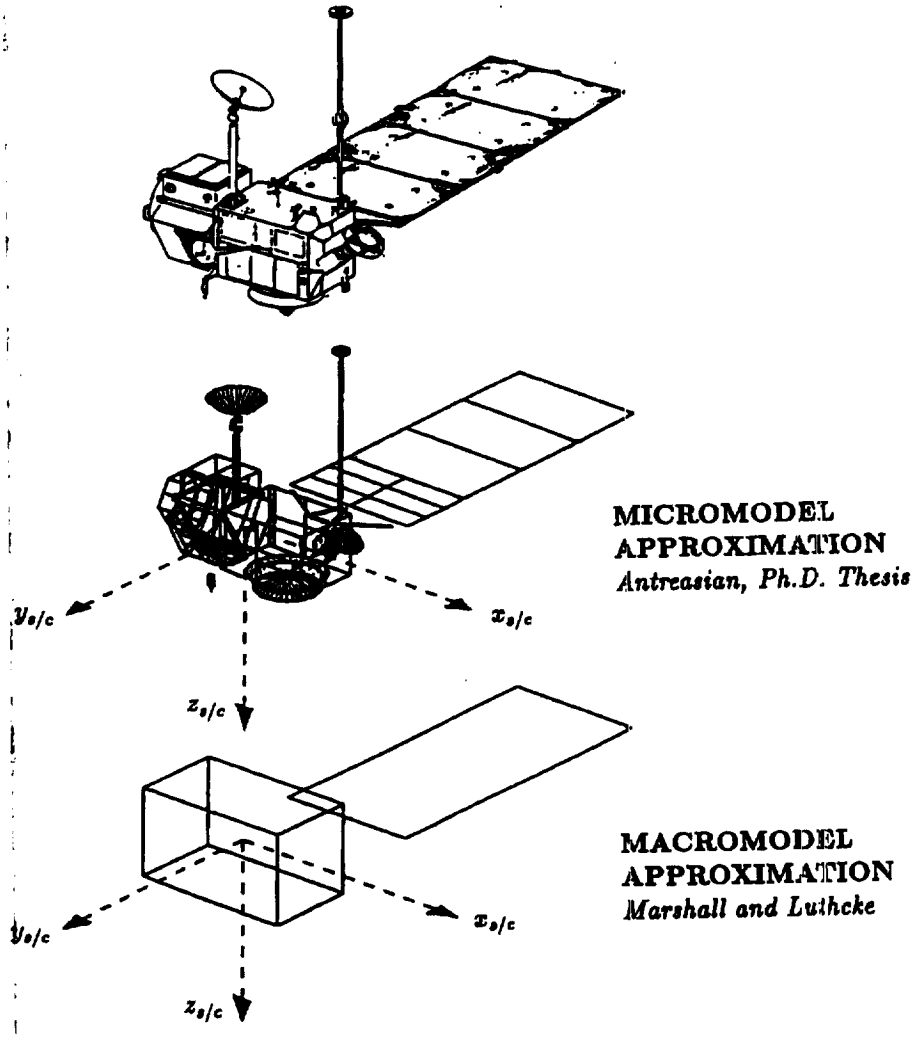

Figure 2 Evolution of the TOPEX/POSEIDON s/c nonconservative force model

The effects of solar array warping have been addressed by Kar and Ries (1993) who show that solar array deflection angles ranging from 3° - 5° can cause alongtrack

accelerations of 0.2 - 0.4 nm/s^2 (1 nm = 1 nanometer = 1x10^{-9} meters) during sinusoidal yaw modes[6].

In order to accommodate the anomalous acceleration, the POD Team tuned (adjusted) the surface property parameters to decrease the root-mean-square (RMS) difference between the computed s/c locations and the observed (via tracking data) s/c location. This was expected to remove most of the mismodeling associated with the simplified macromodel approximation. In addition, constant alongtrack accelerations of 0.38 nm/s^2 and 0.20 nm/s^2 in the $+x_{s/c}$ and $+y_{s/c}$ directions were estimated from the residual alongtrack accelerations and applied throughout the entire 160 day period giving the tuned macromodel results shown in figure 1. This does indeed remove a few of the discontinuities seen at yaw mode transition, but does not change the characteristics seen during sinusoidal yaw periods.

The POD Team was not the only group to observe an anomalous behavior. The T/P Navigation (NAV) Team at NASA's Jet Propulsion Laboratory (JPL) also observed anomalous satellite-fixed accelerations[7]. The NAV Team uses a nonconservative force model which assumes the s/c to be a homogeneous sphere or "cannonball". That model does not account for variations in surface properties or motion of the solar array. Thus, the anomalous satellite-fixed accelerations discussed by Frauenholz *et al.* (1993) are very different from and much larger than the accelerations discussed in this paper.

RADIATION FORCE CALCULATION

The computational model for solar array warping consists of a flat plate, with the properties shown in table 2, which is decomposed into 100 partitions. Nodes are located at the center of each partition. Warping of the solar array results from temperature differences between the front and back surfaces of the solar array and this warping can be quantified using the physical dimensions and the effective coefficient of thermal expansion for the composite solar array[8]. Curvature along the length and across the width of the panel may then be determined for any given temperature difference via the following equation:

$$R = \frac{d}{\alpha_{cte}\Delta T}.$$

Figure 3 shows the compound curvature of the solar array for a temperature difference of 10 K. The resulting tip deflection is approximately 20 cm. For the analysis presented in this paper only curvature along the length of the solar array is considered.

Several MATLAB routines were developed to simulate the T/P orbit, s/c orientation, and compute accelerations due to radiation pressure using s/c position, velocity, temperature, and attitude telemetry which are extracted from the Selected Telemetry Record (STR) files available at JPL. These data are also used to define the important reference frames, determine Earth shadow exit and entry, quantify curvature. The radiation forces acting on the warped solar array are computed and the resulting accelerations are determined in the orbit frame of reference. The difference between the warped solar array accelerations and the flat solar array accelerations is determined and represents the error associated with the assumption that the solar array is flat. The

difference in the alongtrack component was averaged daily over a period covering a β' cycle, similar to the first 160 days of the operational orbit. These days were chosen based upon STR availability at the time.

Table 2
TOPEX/POSEIDON SOLAR ARRAY PHYSICAL CHARACTERISTICS

Definition	Symbol	Value
Length	L	7.72 m
Width	w	3.30m
Thickness	d	0.0349 m
s/c Mass	M	2500 kg
Coefficient of Thermal Expansion	α_{cte}	23.4×10^{-6} K^{-1}
Absorptivity	α	0.80
Reflectivity	γ	0.20
Specularity	β	0.20
Cell SideEmissivity	ε_f	0.81
Back Side Emissivity	ε_b	0.85

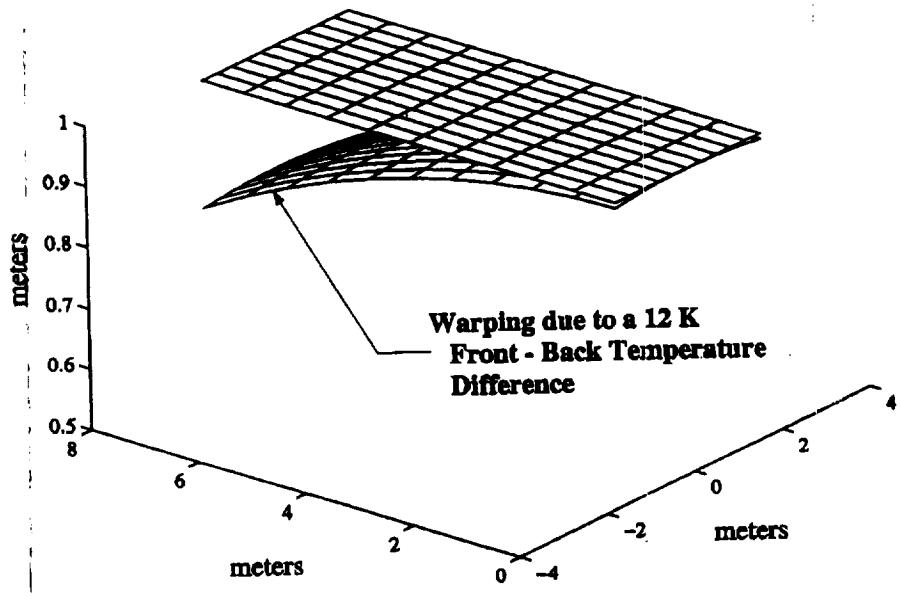

Figure 3 Computational model for solar array warping simulations.

Figure 4 shows the daily average constant alongtrack acceleration due to solar array warping. Examination of the temperature telemetry shows a difference of approximately 10 K – 12 K between the front and back surfaces of the solar array during periods of s/c illumination. According to the warping model used in this analysis, a plane which is

oriented tangent to the center point of the solar array, warped under a 10 K temperature gradient, would be deflected by approximately 1.5°. The resulting daily average alongtrack acceleration is determined to be –0.10 nm/s^2 which is consistent with the results obtained by Kar and Ries (1993).

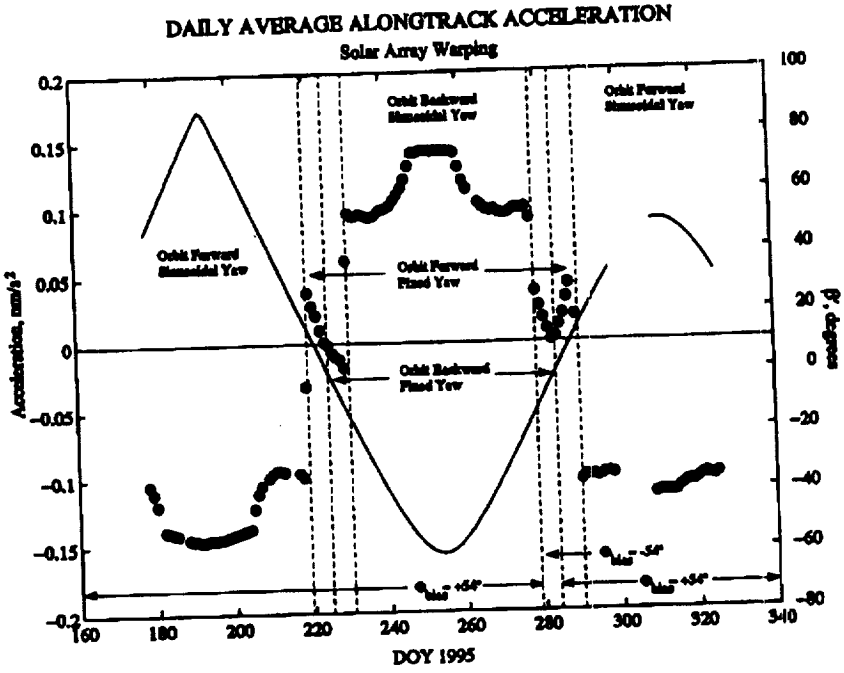

Figure 4 Predicted daily average constant alongtrack accelerations due to solar array warping.

Comparison of the daily average alongtrack acceleration due to solar array warping, with the anomalous acceleration results displayed in figure 1 show similar characteristics during sinusoidal yaw modes. The most promising results are shown during the second orbit forward sinusoidal yaw period (days 290 – 340) where the daily average alongtrack accelerations remain relatively constant. During that period β′ reaches a maximum value of approximately 50° (never experiencing full sun orbits). The β′ values shown in figure 1, which corresponds to the orbit forward sinusoidal yaw period, also do not exceed 55.7° and the associated residual alongtrack accelerations exhibit a constant trend.

Although a comparison of the results obtained from this solar array warping analysis shows similar characteristics throughout the sinusoidal yaw mode regions, it cannot explain the residuals observed during the fixed yaw periods. Also, the magnitude of the alongtrack accelerations due to solar array warping are a factor of three smaller than that of the anomalous acceleration. Nonetheless, these results provide justification enough to proceed with modification of the macromodel being used by the POD Team.

MODIFICATION OF THE TOPEX/POSEIDON MACROMODEL

The original prelaunch and tuned macromodel surface property parameters were used to reconstruct the published anomalous acceleration results, which provided a baseline relative to which changes may be evaluated. Two discrepancies were immediately noted and corrected. The first had to do with the prelaunch macromodel: prior to launch, the T/P solar array design specifications listed the solar array surface area to be 21.4 m^2. That surface area was changed just before launch to the current surface area of 25.5 m^2. The second discrepancy had to do with the tuned macromodel. The tuning process is empirical in nature and can result in unrealistic changes to surface property values. Final values for two of the surface property parameters adjusted during the tuning process exceeded 1.0[9].

It was decided that a four panel approximation of the warped solar array would be used in the modified macromodel approximation as seen in figure 5. A few assumptions have been made in order to simplify the solar array warping model: (1) the solar array is composed of 5052 aluminium honeycomb material, (2) the value for the coefficient of thermal expansion is the value reported in table 2, (3) the curvature across the width of the solar array is neglected, and (4) each of the solar array joints are fully extended and locked in position. The radius of curvature is determined from the equation shown in the previous section and the warped solar array is approximated by first determining the solar array front and back temperatures, next determining the radius of curvature for reorientation of the four subpanels, and finally determining all radiation forces acting on the reoriented subpanels. The necessary modifications were made to create a new GEODYN II module capable of handling the new macromodel, and estimates of the residual alongtrack accelerations were determined over the first 160 days of the operational orbit. Figure 6 indicates that solar array warping alone cannot fully explain the anomalous acceleration during the sinusoidal yaw modes, however, improvements consistent with the results obtained in simulations are seen. The improvements seen during the fixed yaw periods are due to adjustments made to the X+ and X- emissivity values[9].

Solar array deployment angle errors are another possibility since deployment of the solar array could not be guaranteed to better than ±1°. After talking to the design engineers, it was agreed that a 2° deployment deflection angle would not be unrealistic. The GEODYN II macromodel was further modified to include a 2° deflection angle in addition to solar array warping. In other words, the entire structure is rotated about a lateral axis (axis oriented across the width of the solar array) attached to the end of the solar array which is located nearest to the s/c bus. This deflection is assumed to remain constant at all times. The resulting constant alongtrack acceleration estimates are shown in figure 7 and indicate that most of the remaining CAAs during the sinusoidal yaw modes are accounted for. However, a negative mean CAA remains throughout all yaw modes for which no satisfactory explanation has yet been found.

EVALUATION OF THE MODIFIED MACROMODEL

The RMS fits to the tracking data (or the RMS tracking data measurement residuals) are an important quantity when discussing the quality of an orbit solution. The RMS fits

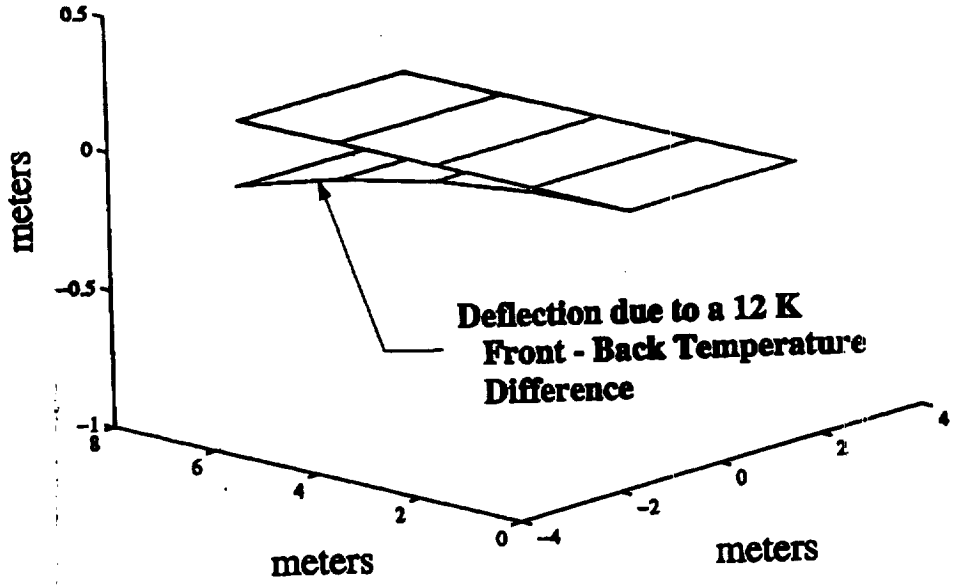

Figure 5 The four panel approximation of solar array warping under a 12 K temperature difference between the front and back surfaces.

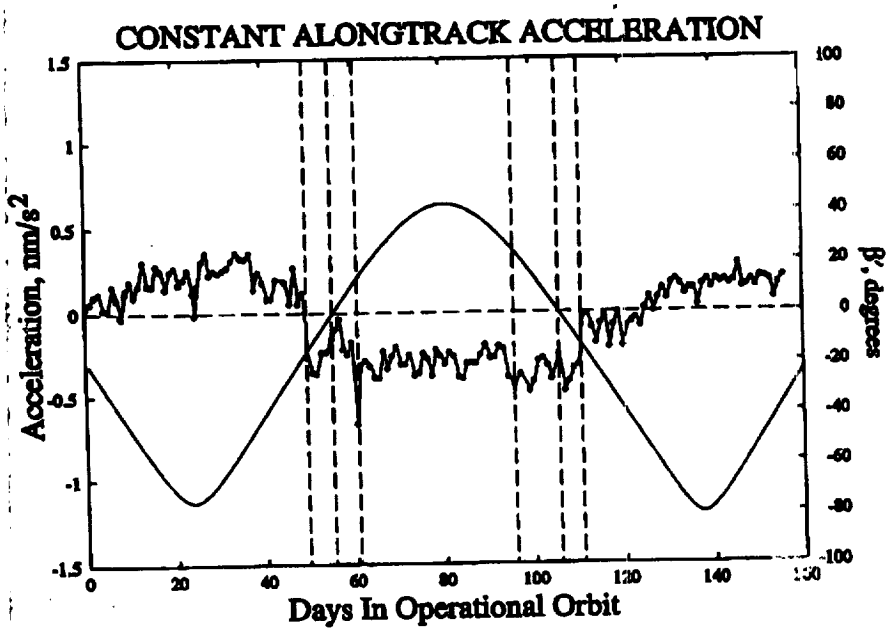

Figure 6 The CAA for solar array warping, X+ emissivity = 0.3, and X- emissivity = 0.9.

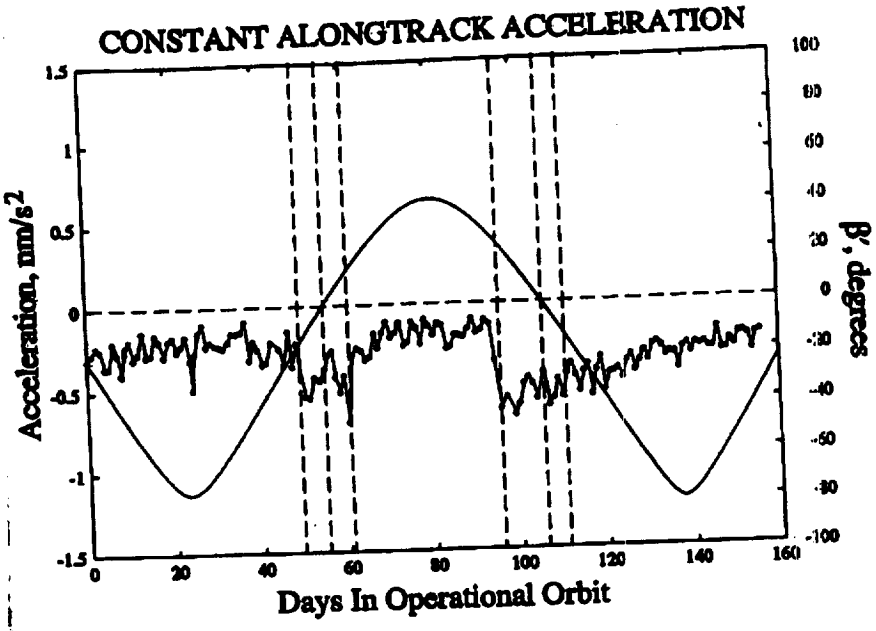

Figure 7 The CAA for solar array warping, a solar array deflection angle of 2°, X+ emissivity = 0.3, and X- emissivity = 0.9.

for both the SLR (satellite laser ranging) and DORIS (Doppler Orbitography Range Integrated System) observations show close agreement for each of the three macromodels[9]. It is important to point out that we would not expect the use of an improved macromodel to result in improved fits to the tracking data since we employ empirical accelerations in all three cases. These empirical acceleration parameters act to absorb unmodeled accelerations. However, we can evaluate the performance of a given macromodel by instead looking at the magnitude of the empirical accelerations. In the case of the modified macromodel, the RMS fits to the tracking data remain unchanged while the magnitude of the CAA parameter is greatly improved through a reduction in magnitude and changes in characteristics.

An important test for validation of the modified macromodel has to do with its performance during later cycles. The empirical constant alongtrack accelerations estimates have been extended through cycle 52. Table 4 shows the statistics over cycles 1-52 for the GSFC tuned macromodel, the modified macromodel which has a solar array deflection angle of 2°, and the modified macromodel which has solar array deflection angle of 1.5°and SA+ diffuse reflectivity of 0.17. The standard deviations shown in table 4 represent the realistic uncertainties in the residual constant alongtrack acceleration values; that uncertainty is 0.16 nm/s^2 for the modified macromodel which uses a solar array deflection of 1.5°.

The dependence of the CAA values on β' were also examined. Figure 8 shows the CAA values as a function of β' and demonstrates that the modified macromodel removes much of the β' dependence.

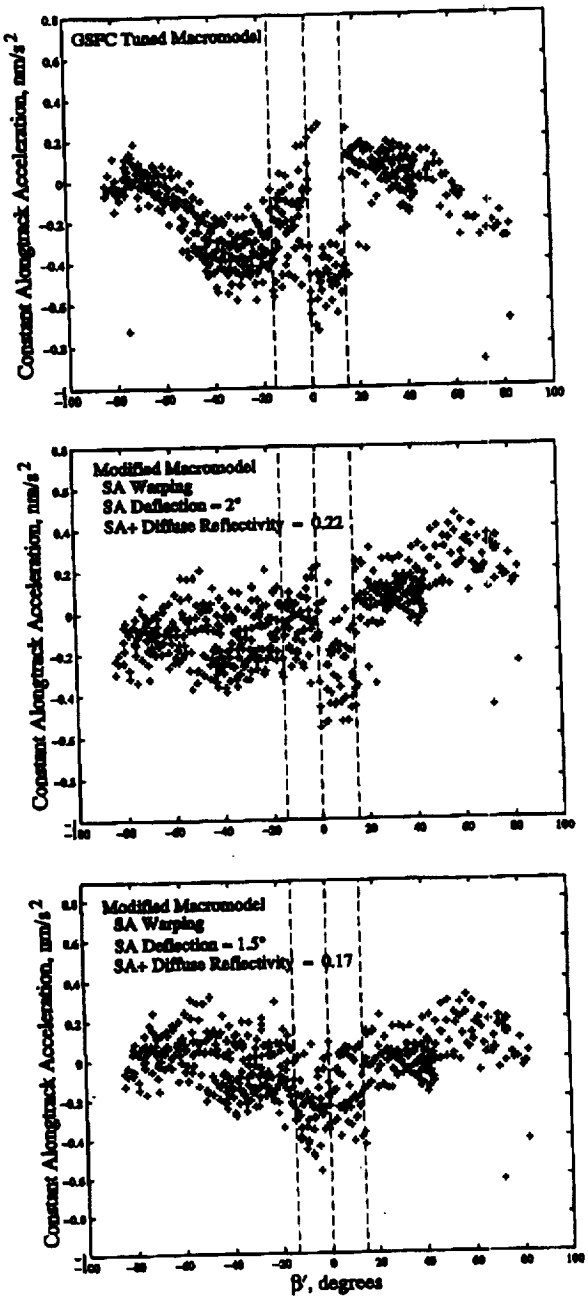

Figure 8 The CAA as a function of β' for three different macromodels during cycle 1-52.

Table 4
CONSTANT ALONGTRACK ACCELERATION STATISTICS FOR THREE DIFFERENT MACROMODELS OVER CYCLES 1-52.

Macromodel	Mean (nm/s^2)	Min (nm/s^2)	Max (nm/s^2)	Standard Deviation (nm/s^2)
GSFC Tuned	-0.158	-0.875	0.549	0.217
Modified 2.0°	-0.042	-0.557	0.466	0.195
Modified 1.5°	-0.036	-0.625	0.321	0.159

MOTION OF THE TOPEX/POSEIDON CENTER OF MASS

The results shown thus far lend support to the hypothesis that warping and a deployment deflection of the T/P solar array may be responsible for the anomalous acceleration. If this is indeed the case, then we must take into consideration motion of the s/c center of mass. The T/P solar array contributes approximately 10% to the entire mass of the s/c. Solar array deflection and solar array warping results in a tip deflection of almost 24 cm. Deflections at the location of the solar array center of mass can be as much as 15 cm which would displace the total s/c center of mass by approximately 1.5 cm. This displacement may be determined as a function of time provided that knowledge of the T/P solar array pitch angle and solar array front and back surface temperatures are available. The MATLAB routines used in the constant alongtrack acceleration simulations were modified to compute the s/c center of mass displacement (or offset) for three characteristic β' regions: (1) high β' during which the s/c is illuminated throughout it's entire orbit, (2) moderate β' during which the s/c is still in the sinusoidal yaw mode, but now it experiences periods of Earth occultation during each orbit, and (3) low β' where the s/c is in the fixed yaw mode with the solar array panel rotating at a frequency of 1 per satellite revolution. Figure 9 shows the displacement of the T/P center of mass in the radial direction. The radial direction is the most important since displacements in the radial component directly affect the altimeter measurements; it is assumed that the center of mass location is known relative to the altimeter measurement reference datum. These computations show that the center of mass can vary by as much as 3 cm in the radial component during fixed yaw. During sinusoidal yaw, the displacement tends to be more characteristic of a negative constant bias. The center of mass offset is determined relative to the s/c frame of reference, so a negative displacement moves the center of mass away from the surface of the Earth. Neglecting this displacement results in altimeter measurements that are short, thus placing the sea surface higher relative to the center of the Earth.

The difficulty now lies in observing the center of mass motion if it exists. Altimeter bias estimates at NASA's primary verification site (Harvest platform) were corrected point by point for the suspected center of mass displacement thinking that this might reduce the standard deviation of the bias estimates. No reduction was observed, however, a shift in the bias estimates of approximately 1-2 cm was seen. This leads to an inclusive result, but provides another example of the importance of understanding this motion and how it affects the altimeter measurements if at all. Using the GEODYN II attitude and temperature model, a time series of the center of mass offset has been computed for cycles 1-121. Figure 10 shows the average, by cycle, center of mass offset for cycles 1-

100. The displacement tends to be negative and correlated with β' as expected. GEODYN II was then modified to accept these offsets for cycle 46 and apply the offset to correct for the location of the center of mass. This led to a degradation in the fits to the tracking data. The SLR RMS of fit changed from 0.0275 m to 0.0283 m. The DORIS RMS of fit was unchanged at 0.0562 cm/s. The magnitudes of the SLR RMS of fits are approximately 2 cm larger than the current state of T/P fits to the tracking data. This is due to the use of early GEODYN setups known as the REPRO-1 setups.

Using the time series information, the center of mass offsets were tied to the T/P reference groundtrack latitude and longitude in an effort to investigate the possibility of a geographic correlation. This data was then transformed to a gridded data set and interpolated to produce a surface representing the error induced by motion of the center of mass. A global map for the each of the first 20 cycles was created and shows features that are latitude dependent during periods of high β' as seen in figures 11 and 12. During the orbit fixed yaw modes there are no latitude dependent features and the center of mass offset appears to be nothing more than a source of noise as seen in figure 13. Figure 14 displays the value of β' over the first 20 cycles.

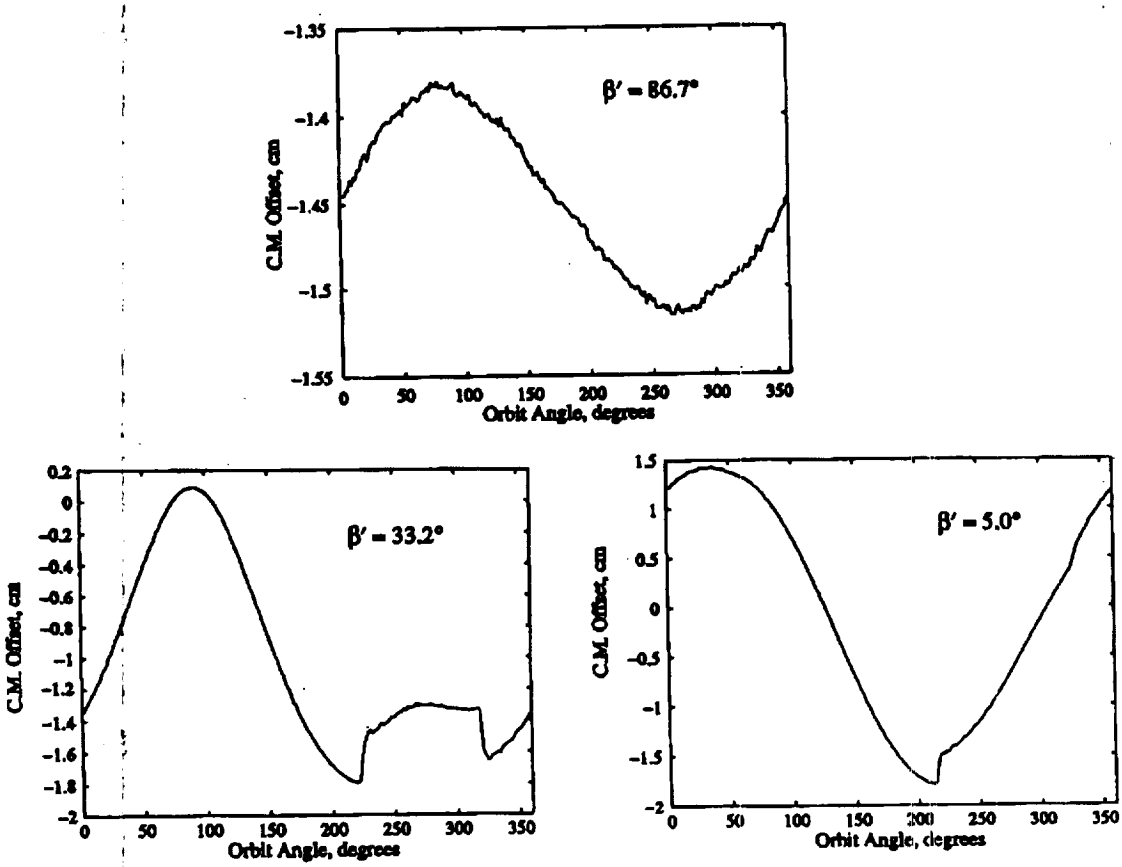

Figure 9 The Radial motion of the TOPEX/POSEIDON center of mass over one orbit revolution due to a 2° solar array deployment deflection and due to solar array warping.

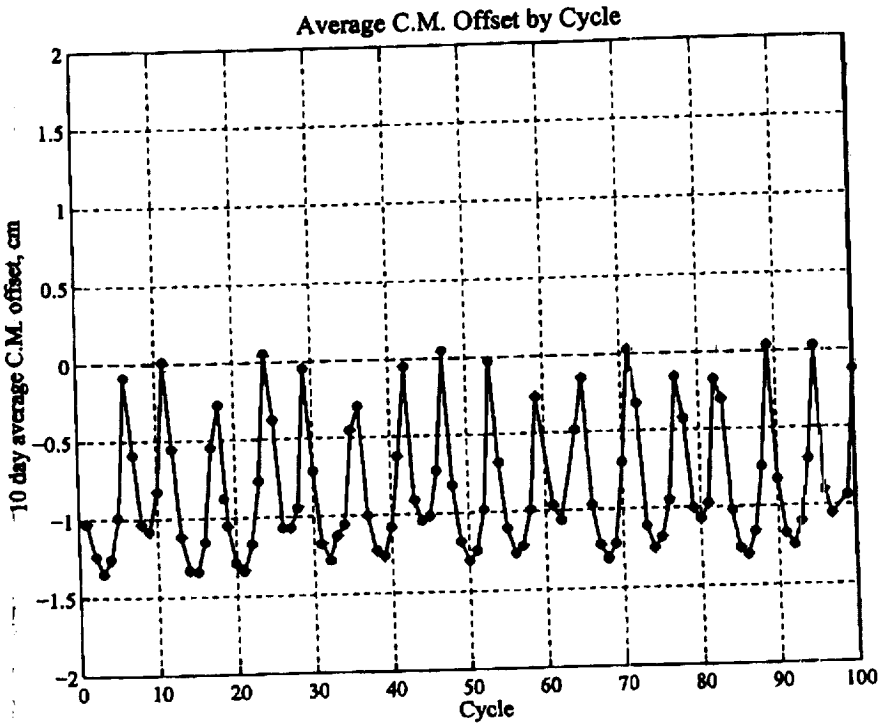

Figure 10 Average cycle by cycle center of mass offset for cycles 1-100.

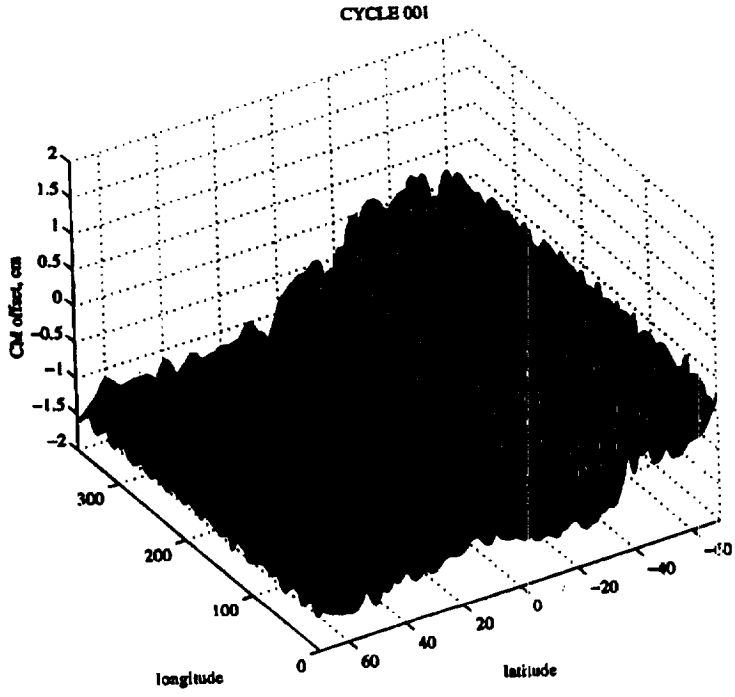

Figure 11 Geographic surface plot for cycle 1 derived from the center of mass offset time series.

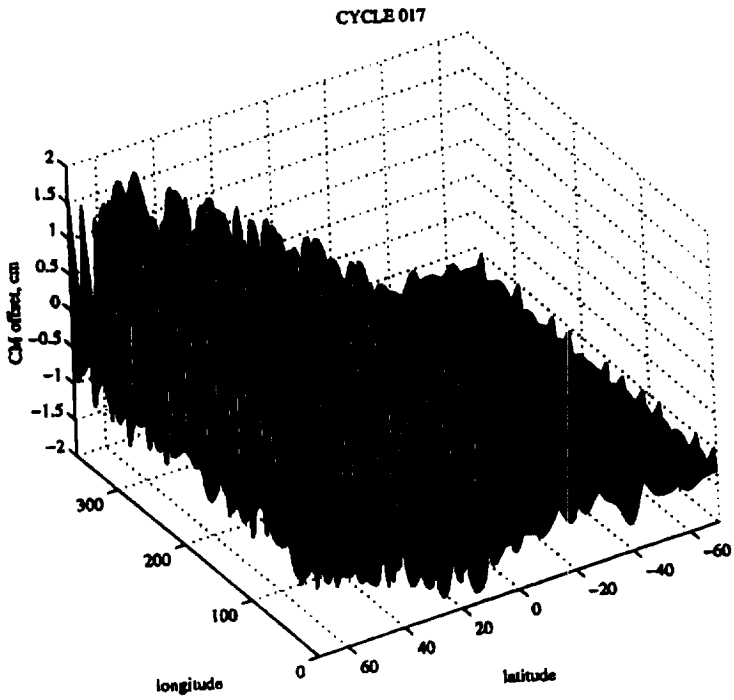

Figure 12 Geographic surface plot for cycle 17.

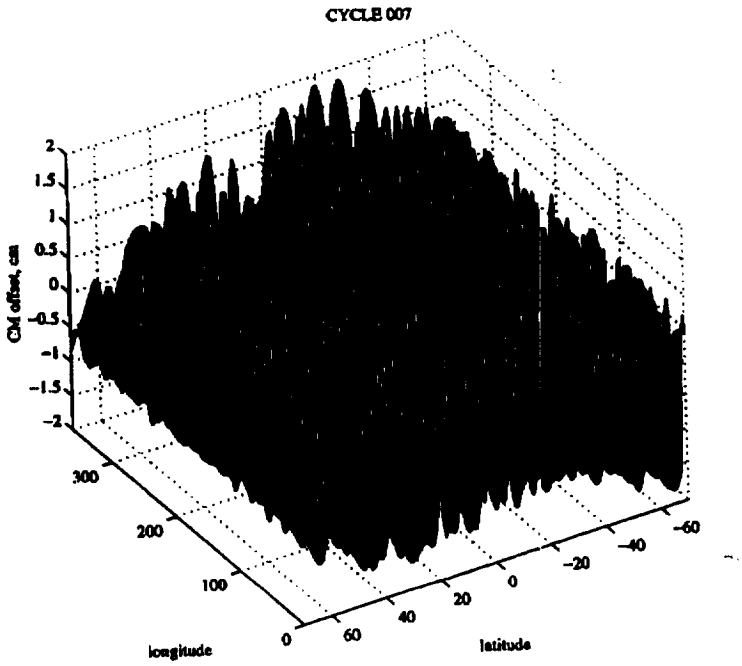

Figure 13 Geographic surface plot for cycle 7.

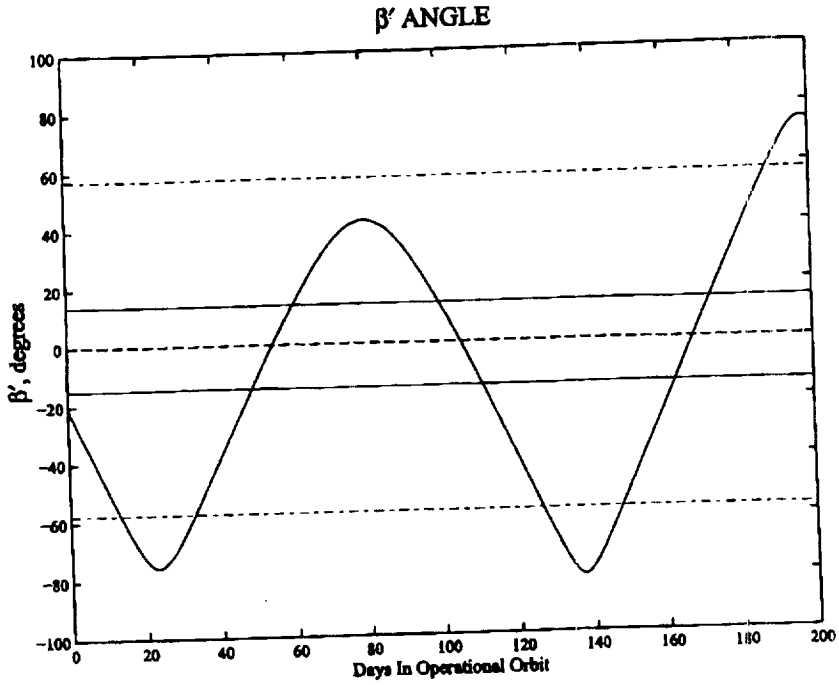

Figure 14 β′ for cycles 1-20.

CONCLUSIONS

The original purpose of the research discussed in this paper was to investigate the anomalous acceleration and provide and explanation for these accelerations. The theory that solar array warping was responsible for the residual constant alongtrack accelerations during the sinusoidal yaw modes was investigated and the results showed that solar array warping alone cannot account for all the residual accelerations. Solar array deployment deflections were then studied showing that deflections of approximately 1.5° - 2° could account for the remaining residual constant alongtrack accelerations during the sinusoidal yaw modes. The anomalous acceleration seen during the fixed yaw modes was removed by adjusting the X+ and X- surface emissivities in the macromodel. It is important to look at the performance of the modified macromodel during later cycles to be sure that the resulting accelerations are improved over a large number of observations. The plot of the estimated constant alongtrack accelerations, shown in figure 8, demonstrate the ability of the modified macromodel to remove much of the β′ dependence. However, if these results are to be believed, then we must look at the effects of solar array motion upon the s/c center of mass. Several attempts have been made to observe this motion: (1) tracking data residuals degrade slightly when the center of mass offsets are included, (2) bias estimates at Harvest platform do not show a clear reduction in standard deviation of the estimates over several cycles, but the center of mass motion would be observed as a systematic error in the altimeter calibrations. Cycle by cycle surface plots, which

represent the center of mass offsets geographically, show some interesting features. These features are on the order of 1-2 cm and may not be observable in the altimetry. It may turn out that this motion has no significant affect upon the T/P altimetry system, but until all possibilities have been exhausted, the question cannot be laid to rest.

ACKNOWLEDGEMENTS

We would like to thank Andy Marshall, Scott Luthcke, and Dave Rowlands; their work set the stage for this research and without their insight and support this research could not have been completed. Thanks goes to Frank Lemoine for his support during the many visits to GSFC over the last several years. Finally, we would like to thank Bob Leben, Chad Fox, and Alex Pufahl for the discussions related to this research and for their help in generating the global surface plots.

REFERENCES

1. Marshall, J. A. and Luthcke, S. B. (1994) "Radiative Force Model Performance for TOPEX/POSEIDON Precision Orbit Determination." *Journal of the Astronautical Sciences*, 49, No. 2, pp. 229-246.
2. Miliani, A., Nobili, A. M., and Farinella, P. (1987) *Non-Gravitational Perturbations and Satellite Geodesy*, Adam Hilger, Bristol.
3. Nerem, R. S. *et al.* (1994) "Gravity Model Developments for TOPEX/POSEIDON: Joint Gravity Models 1 and 2." *Journal of Geophysical Research*, 99, No. C12, pp. 24,421-24,447.
4. Antreasian, P. G. and Rosborough, G. W. (1992) "Prediction of Radiant Energy Forces on the TOPEX/POSEIDON Spacecraft." *Journal of Spacecraft and Rockets*, 29, No. 1, pp. 81-90.
5. Marshall, J. A., Antreasian, P. G., Rosborough, G. W., and Putney, B. H. (1991) "Modeling Radiation Forces Acting on Satellites for Precise Orbit Determination." Paper No. 91-357, *AAS/AIAA Astrodynamics Specialist Conference*, Durango, Colorado.
6. Kar, S. and Ries, J. C. (1993) "The Effect of Solar Array Warping on TOPEX Orbit Determination." *Technical Memorandum CSR-TM-93-02*, Center for Space Research, University of Texas, Austin, Texas.
7. Frauenholz, R. B. *et al.* (1993) "The Role of the Anomalous Satellite-Fixed Accelerations in TOPEX/POSEIDON Orbit Maintenance." Paper No. 93-570, *AAS/AIAA Astrodynamics Specialist Conference*, Victoria, B. C., Canada.
8. Boley, B. A. and Weiner, J. H. (1960) *Theory of Thermal Stresses*, John Wiley & Sons, Inc.
9. Kubitschek, D. G. (1997) "The Anomalous Acceleration and Radiation Force Calculation for the TOPEX/POSEIDON Spacecraft." *Ph.D. Thesis*, Aerospace Engineering Sciences, University of Colorado, Boulder, Colorado.